Energy loss of heavy ions in nuclear collisions in silicon

J. J. Grob, A. Grob, A. Pape, and P. Siffert
Centre de Recherches Nucléaires et Université Louis Pasteur, 67037 Strasbourg Cedex, France
(Received 30 September 1974)

Heavy-ion channeling measurements performed in aligned surface-barrier detectors have allowed the determination of energy losses and straggling in nuclear collisions. Results are presented for $^{28}Si^{+}$ and $^{14}N^{+}$ in the 300–2000-keV region to illustrate the possibilities of this method. Comparisons of the theoretical and experimental data are made. A dependence of the energy partition between electronic and nuclear collisions on the atomic density along the ion path is demonstrated.

I. INTRODUCTION

A heavy charged particle moving through a solid loses its energy (in the keV to MeV range) by screened Coulomb interactions with the substrate atoms. It is usually instructive to distinguish between two energy-loss processes, namely, those by nuclear interactions between the screened nuclear charges and by electronic interactions of the moving ion with bound or free target electrons. For most purposes, this separation into nuclear and electronic collisions, although perhaps not strictly true, represents a good approximation to the observed phenomena.[1] In a given stopping material (of atomic number and mass Z_2, M_2) the first type of interaction is predominant at lower energies (E) or for heavier incident ions (Z_1, M_1), whereas electronic stopping takes over for higher E and lower Z_1 values. The problem of energy partition between both kinds of interactions was considered by Bohr[2] and has more recently received a rather complete theoretical treatment by Lindhard's group.[3–5] From the experimental standpoint the situation is less satisfactory. This results, first, from the absence over a long period of time of heavy-ion accelerators, and second, is due to the lack of a suitable technique permitting the determination of both kinds of energy loss. Mostly, fission fragments have been used as the ion source and solid-state detectors as sensors. For heavy ions a "pulse-height defect" (PHD) appears in these counters, due to the fact that only electronic interactions lead to the creation of electron-hole pairs.[6–8] These alone contribute to the output signal. However, several contributions to the PHD exist, and a precise determination of the nuclear stopping becomes then a delicate problem. To overcome this difficulty, some authors[9,10] bypass the counter dead layer using an (n, n') reaction in a well-defined kinematic situation. This leads to a recoil ion of known energy. Others[11–13] have tried to evaluate and control all the parameters contributing to the PHD.

Here, we propose a more general and precise method to evaluate both the energy loss by nuclear collisions and its fluctuation. This method is valid for any Z_1, M_1 ion absorbed in a crystalline solid-state detector (currently silicon, germanium, diamond[14] and cadmium telluride[15]). In order to demonstrate the capabilities of this procedure, we have made measurements on $^{28}Si^{+}$ and $^{14}N^{+}$ ions stopped in silicon. This procedure is based on the fact that a heavy ion moves through certain regions of a crystal (main crystallographic axes) without close collisions with the atoms forming the "walls" of the "channels," and consequently without nuclear interactions in the case of well-channelled ions.[16] In this experimental situation the measurement of pure electronic stopping is possible without interference from nuclear recoils.

II. EXPERIMENTAL

A. Accelerator

A heavy-ion source has been specially designed and installed in the terminal of the Strasbourg 2-MV Van de Graaff accelerator. The details of this equipment have been described elsewhere.[17]

In the case of the $^{28}Si^{+}$ beam obtained from silane, a differentially pumped gas stripper broke up accelerated SiH_3^{+} fragments after a first analyzing magnet. A second magnet allowed selection of isotopically pure beams. The energy of the ions ranges between 300 and 2000 keV. The calibration in energy of the machine was achieved through a well-known $^{27}Al(p, \gamma)\,^{28}Si$ resonance.

B. Heavy-ion detection

When heavy ions of energy E_0 are detected in a silicon-surface-barrier detector, a PHD ΔE appears (when compared to protons of identical energy) given by

$$\Delta E = \Delta E_W + \Delta E_R + \nu(E_0 - \Delta E_W) \ , \qquad (1)$$

where ΔE_W is the energy lost in the dead layer of the detector (gold film and possible silicon or oxide layer),[18,19] ΔE_R the ionization defect due to charge recombination and carrier trapping in the depletion region of the counter, and $\nu(E_0 - \Delta E_W)$

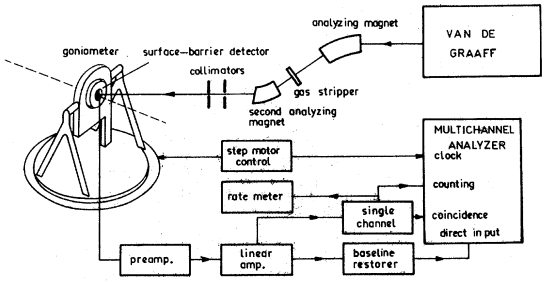

FIG. 1. Schematic diagram of the experimental setup.

the energy lost through nonionizing nuclear processes. The detectors were fabricated in our laboratory by evaporating thin gold layers of known thickness (100–400 Å) onto 150-Ω cm n-type ⟨111⟩-oriented silicon wafers after correct surface etching. By choosing low-resistivity materials and high bias voltages, the electric field in the depletion zone is high enough to reduce the recombination probability to a negligible value ($\Delta E_R \approx 0$). The energy resolution of these counters ranged between 12 and 17 keV for 5.5-MeV α particles. Relation (1) supposes that the number of any x rays escaping the depletion layer of the diode is negligible.

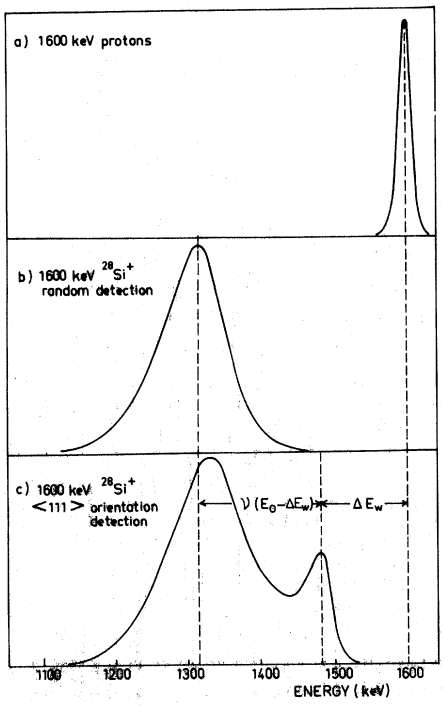

FIG. 2. Spectra recorded for (a) protons, (b) unchanneled $^{28}Si^+$ ions, and (c) $^{28}Si^+$ ions channeled along the ⟨111⟩ crystal axis. The ion energy in each case was 1600 keV. The detector was made from 150-Ω cm resistivity silicon and was biased at 700 V.

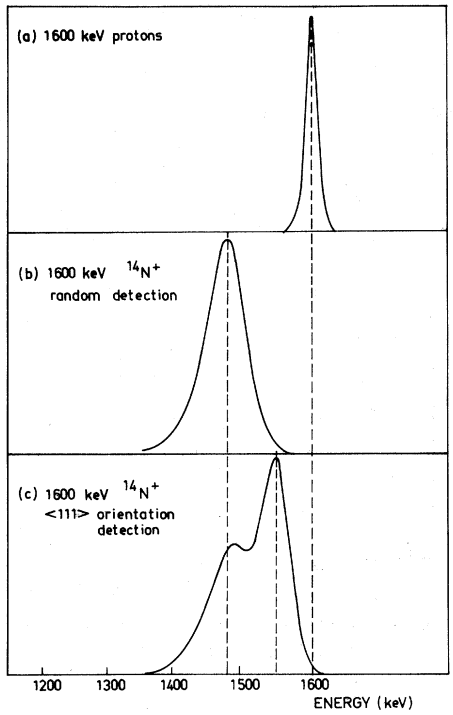

FIG. 3. Spectra recorded for (a) protons, (b) unchannelled $^{14}N^+$ ions, and (c) $^{14}N^+$ ions channeled along the ⟨111⟩ crystal axis. The ion energy in each case was 1600 keV. The detector was made from 150-Ω cm resistivity silicon and was biased at 450 V.

C. Apparatus and procedure

The detector was mounted in a high-precision three-axis step-motor-controlled goniometer placed in an evacuated ($p \approx 10^{-6}$ torr) target chamber. The beam impinged directly on the detector. The intensity of the beam was reduced to less than 10^{-13} A by means of very small apertures (≈0.3-mm diam) to reduce the counting rate. Using collimators of different diameter produced no changes in the form of the spectra and showed that collimator-edge effects were negligible. The signal delivered by the counter after conventional amplification was analyzed in a multichannel system. Pulse pile up was reduced by restorer-rejector electronics. The energy calibration of the detection system was performed by protons.

The alignment of the detector crystal axes along the beam axis was done by making use of the fact that the PHD diminishes when the ions enter the crystal along atomic planes. Making a scanning around an axis, we observed the apparition of a channelled peak every time the ions penetrated the crystal parallel to a plane. A schematic diagram of the experimental setup is shown in Fig. 1.

III. RESULTS AND DISCUSSION

Figure 2 shows spectra recorded for protons

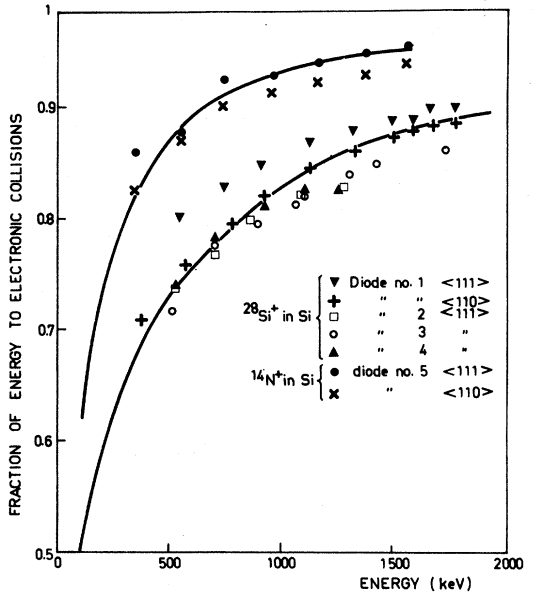

FIG. 4. Fraction of energy deposited by electronic stopping for $^{28}Si^+$ and $^{14}N^+$ ions in silicon.

[Fig. 2(a)], and for $^{28}Si^+$ ions of equal energy in a random orientation [Fig. 2(b)] and oriented along the ⟨111⟩ axis [Fig. 2(c)]. In the aligned-detection condition two peaks are present, whereas in the random condition only one broad peak appears for $^{28}Si^+$ ions. The higher-energy "aligned" peak does not correspond to the energy position of the proton distribution of identical energy E_0. The difference is due to the energy lost by the $^{28}Si^+$ in the entrance window of the detector (ΔE_W). Thus, the energy of the heavy ions entering the depletion region is $(E_0 - \Delta E_W)$ and the corresponding nuclear-energy losses $\nu(E_0 - \Delta E_W)$ are given by the difference in energy between the "aligned" and the "random" peak [Fig. 2(c)]. Similar results are found (Fig. 3) for $^{14}N^+$ ions detected along the ⟨111⟩ axis of another detector.

A. Nuclear-collision energy losses

From the analysis of the PHD for $^{28}Si^+$ and $^{14}N^+$ ions as a function of energy, it is possible to construct the curves of Fig. 4 which show the energy dependence of the ionization produced by these ions relative to protons of equal incident energy. The full lines are calculated from Lindhard's model.[3–5] The experimental points are in rather good agreement with these predictions. The slight scatter in the experimental points results from the use of detectors biased at different voltages, and also from different atomic densities encountered by the projectile along the ⟨111⟩ and ⟨110⟩ lattice axes (see Sec. III C).

In order to compare our results with previously published data,[6–13] we have plotted the nuclear-energy losses $\nu(\epsilon)$ versus the reduced energy ϵ (as defined by Lindhard) in Fig. 5. Solid lines are the calculations of Lindhard for $k = 0.1$ and $k = 0.2$, and the dashed line, those of Haines and White-

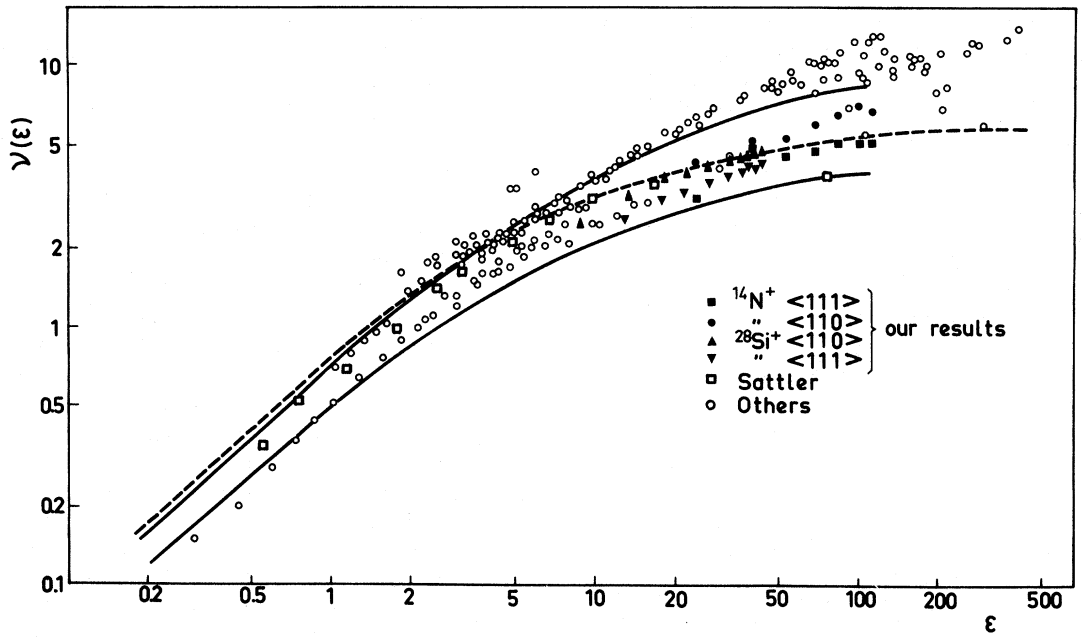

FIG. 5. Resumé of available data for energy lost by heavy ions by nuclear collisions in silicon in terms of reduced variables ν and ϵ. Data points are from the present work and Refs. 6–13. The two solid lines are the theoretical curves of Lindhard *et al.* (Ref. 5) for $k = 0.1$ and 0.2. The dashed curve is the theory of Haines and Whitehead (Ref. 20).

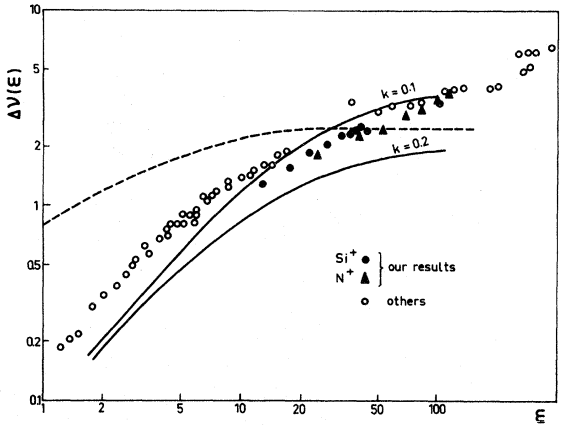

FIG. 6. Resumé of available data on energy straggling for heavy ions in nuclear collisions in silicon in terms of the reduced variables ν and ϵ. Data points are from the present work and Refs. 6–13. The solid curves are the theoretical curves of Lindhard *et al.* (Refs. 3–5) for $k=0.1$ and 0.2. The dashed curve is the theory of Haines and Whitehead (Ref. 20).

head.[20] In spite of the fact that all available experimental points are approximately confined between the two solid lines of theory, a very important dispersion appears in the results. Specifically, the mass dependence of the nuclear stopping is not apparent when the points are expressed in terms of reduced variables. Detailed analysis of the experimental results in the literature indicates that three errors in nuclear stopping evaluations are often made.

(i) The main error arises from the estimation of the energy lost in the dead layer of the detector. Generally, this contribution is estimated from the knowledge of the stopping cross section of the incident ion in gold. But, as will be shown below, gold does not constitute the only contribution to the window, and, moreover, the structure of the film is not necessarily that of films prepared by other techniques. In fact, a gold layer of less than 200–300-Å thickness possesses a granular structure with large open areas.[21] Therefore, the average thickness is of little significance, as shown[22] from low-energy x-ray transmission measurements. In our procedure, the energy loss in the entrance window is measured directly. Consequently, we observe that our results are in close agreement with Sattler's data,[9,10] which was measured using silicon recoil atoms from (n,n') reactions and which is independent of any window effect. These data agree well with theoretical estimations for $k=0.15$ ($k_{Si}=0.146$).

(ii) A second source of error can result from incomplete charge collection of the generated electron-hole pairs formed in the detectors. We suppose that this effect is minimized when biasing the detectors at a voltage sufficient to reach the saturation plateau of pulse amplitude for the heavy ion considered.

(iii) A third possible error can result from an "anisotropy" of the atomic density and which has for effect that the nuclear stopping contribution depends on the angle at which the ions penetrate the counter. This effect, which has been found to be important, will be considered in detail below.

B. Energy dispersion due to nuclear collisions

The peak width L[Fig. 2(b)] obtained under random bombardment is assumed to be given by

$$L^2=L_W^2+L_R^2+L_\nu^2 \ ,$$

where L_W is the energy straggling of the ion beam in the dead layer, L_R the dispersion due to incomplete charge collection, and L_ν the nuclear-collision contribution.

When the particles are channeled, the term L_ν disappears and the width of the peak is reduced to L_W if we neglect recombination and fluctuation in the charge-carrier creation. In other words, the energy dispersion due to nuclear processes L_ν^2 is given by the quadratic difference between the observed widths of the random and channeled peaks.

The results, plotted as a function of the dimensionless units are reported in Fig. 6. On the same figure are shown the theoretical estimations of Lindhard[3–5] and Haines and Whitehead.[20]

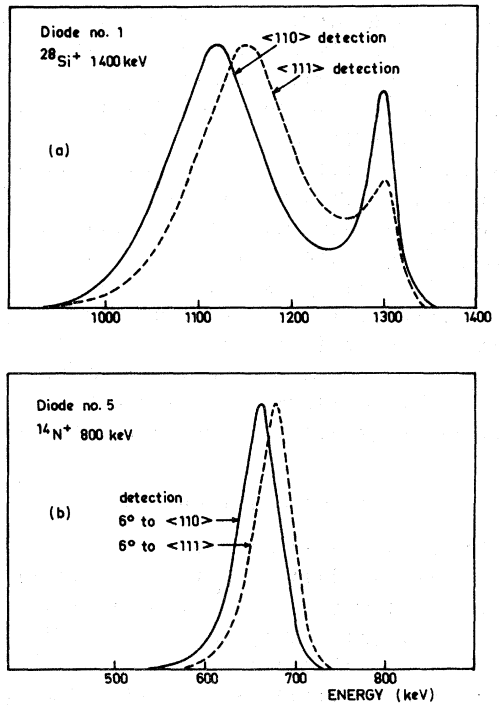

FIG. 7. Influence of the incident ion direction on the PHD in an (a) aligned and (b) random case.

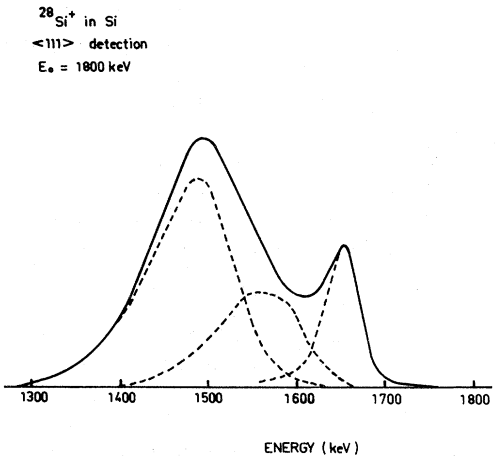

FIG. 8. Decomposition (dashed curves) of an aligned spectrum into totally channeled and totally unchanneled components. The contribution in the middle is presumably due to initially channeled ions which become dechanneled along their path.

C. Atomic-density effect on nuclear collisions

One of the most interesting results of this work is that the energy lost in nuclear collisions is dependent on the orientation of the ion trajectory in the crystal. This result, visible on Figs. 4 and 5, becomes more apparent in Fig. 7. Even for a random-ion detection [Fig. 7(b)], if the incident direction is not too far away from a major axis, the different densities of lattice atoms encountered by the projectile involve substantial variation in the nuclear energy losses. A tentative explanation is as follows. For the simplified picture of a uniform electron gas within the solid, the electronic stopping per unit distance is independent of the projectile direction. However, the frequency of nuclear encounters per unit distance depends on the atomic density along the trajectory of the projectile, and the fractional energy loss due to nuclear stopping thus also depends on projectile direction. Experimentally, this is the first time, as far as we know, that this "anisotropy" has been seen, and as noted in Sec. III A, can introduce errors in the evaluation of the energy partition between electronic and nuclear collisions.

D. Influence of channeling

The influence of several parameters on the number of channeled heavy ions in the detectors has been investigated. First, it has to be pointed out that in the aligned configuration, the position of the left-most peak of an energy spectrum does not coincide exactly with the "pure" random peak position [see Figs. 2(b) and 2(c) and 3(b) and 3(c)]. This is due to a distortion of the random peak by a partly channeled component. Consequently, the real contribution of the random peak in the aligned spectrum had to be obtained from a fit of the true random form to the low-energy side of the random part in the aligned spectrum. Using such a normalization, we split up the aligned spectrum into three components (Fig. 8):

(a) The lowest-energy peak, or "random" peak, corresponding to ions which are never channeled. Its width is determined mostly by fluctuations in nuclear energy losses.

(b) The peak located at the highest energy, or the "aligned peak", corresponding to ions that remain channeled throughout their entire range. This peak is relatively narrow, its width determined by the energy dispersion in the dead layer (noise and statistical fluctuation of electronic charge generated being of minor importance here).

(c) The intermediate-energy peak presumably corresponding to ions which are initially channeled and subsequently dechanneled (by defects, thermal vibrations, etc.). The large width of this distribution is due to dechanneling at different points along the ion path.

It can be seen from the data that the relative number of channeled ions depends on mass (Figs. 2 and 3), energy [Fig. 9(a)], and on the axis followed by the particle [Fig. 9(b)]. The greatest single factor in determining the fraction of channeled incident ions is the thickness of the gold layer. For example, in the case of $^{28}Si^+$ ions crossing a 150-Å-thick gold layer, the beam divergence reaches 2° at 600 keV and 0.5° at 1900 keV.[23]

IV. CONSIDERATIONS ON DETECTOR ENTRANCE WINDOW

The real window thickness of silicon-surface-barrier detectors has been under study for several

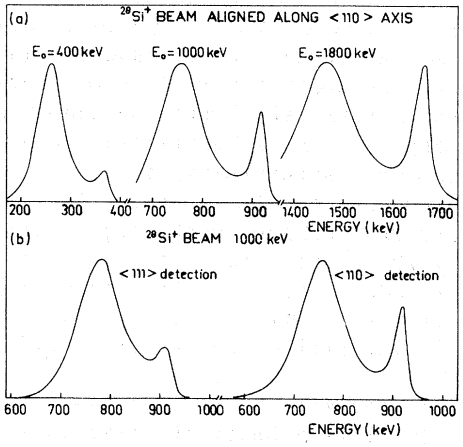

FIG. 9. Dependence of the channeled fraction on (a) incident-ion energy and (b) crystal axis.

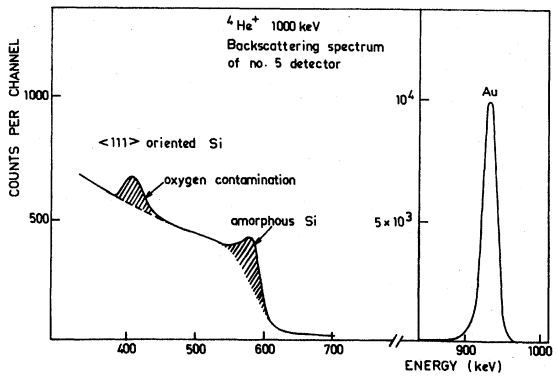

FIG. 10. Spectrum at 130° of 1-MeV α-particles backscattered from detector No. 5.

years[18,19] and has not yet been completely explained. In all the detectors we have used, the measured energy losses ΔE_W in the window are too large to be due to the deposited gold layer alone. As an example, with 1-MeV $^{28}Si^+$ ions, the observed energy loss in the window is about 100 keV, corresponding to 500 Å of gold (as deduced from theoretical energy-loss estimations[24]). This is much thicker than the deposited gold layer. In order to clarify this point, we performed a $^4He^+$ back-scattering experiment to determine the thickness and composition of the surface layer of our surface-barrier counters. Using the $^4He^+$ stopping power in gold,[24] we found that the mean gold layer thickness is only 145 ± 25 Å. When the helium beam was aligned with the ⟨111⟩ or ⟨110⟩ axial directions, no change attributable to other than an angle dependence was observed. So the gold layer is either amorphous or the orientation of its crystallites is sufficiently random to allow the treatment of these films as amorphous structures. The back-scattering spectrum (Fig. 10) shows a rather broad oxygen distribution close to the surface. The width of this oxygen peak is found to be approximately 400 Å. The oxygen yield could not be precisely determined, but it seems certain that the oxygen concentration is much less than enough to correspond to an SiO_2 stoichiometry. If this 400 Å is composed to a quasiamorphous silicon layer containing a small amount of dissolved oxygen so that the carrier lifetime is short, and the energy losses of the incident ions in 150 Å of gold and 400 Å of silicon are added together, the sum agrees approximately with the observed energy loss in the window (Fig. 11). It is clear that these numerical values are valid only

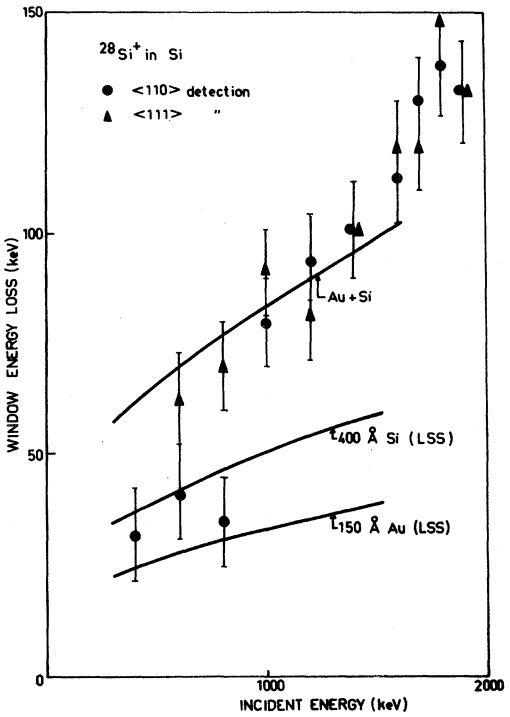

FIG. 11. Energy loss of $^{28}Si^+$ ions in the detector entrance window as a function of incident $^{28}Si^+$ energy. The solid curves are energy losses calculated from the theory of Lindhard, Scharff, and Schiøtt (Ref. 4).

for detectors prepared by our manufacturing technique. Other conditions may lead to different results.[25]

V. CONCLUSION

The experiments reported here show that the detection of heavy ions by a silicon solid-state detector in a channeling direction allows, first, the measurement of the PHD and energy straggling due to nuclear collisions, and second, the energy loss and straggling in the detector entrance window.

Our experimental results agree with Lindhard's theoretical calculations and point out that the different atomic densities along different penetration directions lead to substantial changes in the nuclear energy losses.

Such experiments as these promise to be of great interest as a new tool in energy-loss studies, channeling of heavy ions, and in the technology of heavy-ion detection devices.

[1]J. Lindhard, Mat. Fys. Medd. Dan. Vid. Selsk. 28, No. 8 (1948).
[2]N. Bohr, Mat. Fys. Medd. Dan. Vid. Selsk. 18, No. 8 (1954).
[3]J. Lindhard, V. Nielsen, and M. Scharff, Mat. Fys. Medd. Dan. Vid. Selsk. 36, No. 10 (1968).
[4]J. Lindhard, M. Scharff, and H. E. Schiøtt, Mat. Fys. Medd. Dan. Vid. Selsk. 33, No. 14 (1963).
[5]J. Lindhard, V. Nielsen, M. Scharff, and P. V. Thomsen, Mat. Fys. Medd. Dan. Vid. Selsk. 33, No. 10

(1963).
[6]W. W. Walker, C. D. Moak, and J. W. T. Dabbs, Bull. Am. Phys. Soc. 10, 515 (1965).
[7]G. Forcinal, P. Siffert, and A. Coche, IEEE Trans. Nucl. Sci. NS-15, 475 (1968).
[8]J. A. Ray and C. F. Barnett, IEEE Trans. Nucl. Sci. NS-16, 82 (1969).
[9]A. R. Sattler, Phys. Rev. 138, 1815 (1965).
[10]C. Chasman, K. W. Jones, R. A. Ristinen, and J. T. Sample, Phys. Rev. 154, 239 (1967).
[11]T. Karcher and N. Wotherspoon, Nucl. Instrum. Methods 93, 519 (1971).
[12]B. D. Wilkins, M. J. Fluss, S. B. Kaufman, C. E. Gross, and E. P. Steinberg, Nucl. Instrum. Methods 92, 381 (1971).
[13]R. D. Campbell and R. P. Lin, Rev. Sci. Instrum. 44, 1510 (1973).
[14]S. F. Kozlov, E. Belcarz, M. Hage-Ali, R. Stuck, and P. Siffert, Nucl. Instrum. Methods 117, 277 (1974).
[15]R. Triboulet, Y. Marfaing, A. Cornet, and P. Siffert, J. Appl. Phys. 45, 6 (1974).
[16]L. Eriksson, J. A. Davies, and P. Jespergaard, Phys. Rev. 161, 219 (1967).
[17]J. Denimal, H. Gasser, and C. Ricaud, Nucl. Instrum. Methods 114, 93 (1974).
[18]G. Forcinal, P. Siffert, and A. Coche, *Semiconductor Nuclear Particle Detectors and Circuits* (National Academy of Sciences, 1969), edited by W. L. Brown, W. A. Higinbotham, G. L. Miller, and R. L. Chase, Publication No. 1593, p. 37.
[19]N. J. Hansen, Nucl. Instrum. Methods 96, 373 (1971).
[20]E. L. Haines and A. B. Whitehead, Rev. Sci. Instrum. 37, 190 (1966).
[21]K. L. Chopra, *Thin Film Phenomena* (McGraw-Hill, New York, 1969).
[22]H. Lipson, K. E. Singer, J. Phys. C 7, 12 (1974).
[23]L. Meyer, Phys. Status Solidi B 44, 253 (1971).
[24]J. A. Borders, Radiat. Eff. 16, 253 (1972).
[25]E. Elad, C. N. Inskeep, R. A. Sareen, and P. Nestor, IEEE Trans. Nucl. Sci. NS-20, 534 (1973).